



Queensland University of Technology
Brisbane Australia

This is the author's version of a work that was submitted/accepted for publication in the following source:

Tao, Qi, Zhu, Jianxi, Wellard, R. Mark, Bostrom, Thor E., Frost, Ray L., Yuan, Peng, & He, Hongping (2011) Silylation of layered double hydroxides via an induced hydrolysis method. *Journal of Materials Chemistry*, 21, pp. 10711-10719.

This file was downloaded from: <http://eprints.qut.edu.au/43345/>

© Copyright 2011 Royal Society of Chemistry

Notice: *Changes introduced as a result of publishing processes such as copy-editing and formatting may not be reflected in this document. For a definitive version of this work, please refer to the published source:*

<http://dx.doi.org/10.1039/C1JM10328H>

Silylation of Layered Double Hydroxides via an Induced Hydrolysis Method†

Qi Tao,^{a,b} Jianxi Zhu,^a R. Mark Wellard,^b Thor E. Bostrom,^b Ray L. Frost,^{*b} Peng Yuan,^a and Hongping He^{*a,b}

5

A series of layered double hydroxides (LDHs) based composites were synthesized by using induced hydrolysis silylation method (IHS), surfactant precursor method, *in-situ* coprecipitation method, and direct silylation method. Their structures, morphologies, bonding modes and thermal stabilities can be readily adjusted by changing the parameters during preparation and drying processing of the LDHs. The characterization results show that the direct silylation reaction cannot occur between the dried LDHs and 3-aminopropyltriethoxysilane (APS) in an ethanol medium. However, the condensation reaction can proceed with heating process between adsorbed APS and LDHs plates. While using wet state substrates with and without surfactant and ethanol as the solvent, the silylation process can be induced by hydrolysis of APS on the surface of LDHs plates. Surfactants improve the hydrophobicity of the LDHs during the process of nucleation and crystallization, resulting in fluffy shaped crystals; meanwhile, they occupy the surface –OH positions and leave less “free –OH” available for the silylation reaction, favoring formation of silylated products with a higher population in the hydrolyzed bidentate (T²) and tridentate (T³) bonding forms. These bonding characteristics lead to spherical aggregates and tightly bonded particles. All silylated products show higher thermal stability than those of pristine LDHs.

20 Introduction

Silylation, also known as silane grafting, has been proven an efficient method to modify the surfaces of inorganic materials including glass, silicon chips, metals and clays¹⁻⁶. The abundant hydroxyl groups on the solid surface can condense with silanes to form Si–O–Si networks. The resultant materials have important applications in chromatography, as antimicrobial agents, catalysts, supports for enzymes immobilization, and fiber reinforced composites⁷. More recently, grafting clays with silanes has attracted great interests since the resultant silylated-clays can significantly improve the affinity between clays and polymer, resulting in great improvement of the properties of the clay-based composites^{1, 3, 4, 7-9}. However, most of these researches focused on cationic clay minerals, for example, smectite group minerals and minerals from the serpentine group^{1, 35}. Very few studies were conducted on the grafting silane onto the surface of layered double hydroxides (LDHs), the only anionic clay mineral existing in nature^{10, 11}. The most important reason rests on their higher surface charge density (about one positive charge per 25 Å² for the case of n_{Mg}/n_{Al}=0.32)¹² compared with other clays (e.g. the unit cell charge of smectite clays varied from –0.6 to –1.4 per O₂₀ unit)¹³. Such a problem can be overcome using surfactants to improve the hydrophobicity of the surface of LDHs and introduce silane molecules to reach and condense with the surface –OH groups.

LDHs have the same structure and properties as natural hydroxylated (Mg₆Al₂(OH)₁₆(CO₃)·mH₂O), but they are synthesized in the laboratory. The Mg²⁺ in its brucite-like octahedral plate is partly substituted by Al³⁺, and the resultant excess charge is balanced by the interlayer anionic ions. The unique positive layers and excellent anion exchange characteristics result in a wide variety of applications as adsorbents, ion exchangers, pharmaceuticals, catalysts etc¹⁴⁻²⁰.

Just like the other solid materials, a compatibility problem between the hydrophilic LDHs and the hydrophobic polymer will be encountered when LDHs are dispersed into polymer matrix. One resolution is to modify the LDHs surfaces with organic surfactants and/or coupling agents to change the hydrophilic surfaces of LDHs to hydrophobic. Silylation is the most common process, especially when organosilanes have nucleophilic groups (e.g. 3-aminopropyltriethoxysilane, APS)^{10, 11, 21-25}. In this case, organosilane can not only increase the hydrophobicity of substrates by the surface grafting, but also help to bond with the polymers via amino groups. Furthermore, the exfoliation of LDH layers may occur during grafting²⁶, which is very important in improving the mechanical property of the resultant clay-based composites.

Different mechanisms have been reported in the literature for silylation processes in different solvents. It is generally observed that, in most nonaqueous solutions, the silylation reaction cannot occur directly and silane molecules can only be physisorbed to the surface of the solid. While in aqueous solution the silanes undergo hydrolysis and preorganization prior to condensation with solid surface hydroxyl groups, to form dimerized chains^{27, 28}. In our previous work, the later mechanism is evidenced by showing the variation of signal locations and populations in ²⁹Si NMR spectra between non- and aqueous solutions²⁹.

Park *et.al* reported for the first time a covalent bonding formed between LDHs and silane¹⁰. A two-step approach was taken to obtain silylated LDHs in their study. The dodecylsulfate (DS) intercalated LDHs was prepared firstly; and then APS was added into the reaction system together with *N*-cetyl-*N,N,N*-trimethylammonium (CTAB). The hydrophobic salts formed from these two kinds of oppositely charged surfactants, which would be replaced by APS and lead to the silylated LDHs. Shortly afterwards, Wypych *et.al* successfully synthesized the single-layer LDHs silylated products¹¹. They also proved the resultant samples can be used as a catalyst after iron porphyrin

immobilized. More recently, our group developed the *in-situ* coprecipitation method and the calcination-rehydration method to graft silanes onto the surface of LDHs. In our studies, the influences of the content of surfactant on the structures, morphologies, and thermal properties of the final silylated samples were discussed based upon these water abundant reaction system^{26, 29}. However, from the literatures mentioned above, a conclusion can be drawn that it is difficult to precisely control the type of bonding in the silylation products.

Herein, we report an initial attempt to adjust the properties of silylated products by grafting water-rich LDHs in ethanol (induced hydrolysis silylation method, IHS). As the comparisons, samples were also collected in aqueous solution by *in situ* coprecipitation silylation method²⁶, and in ethanol by precursor silylation method to graft the water-rich surfactant-modified LDHs. For a better understanding the key factors during silylation reaction, the contents of surfactant were controlled to avoid their intercalation into the LDHs, which is different from the previous report³⁰. By using these measures, clay based composites can be obtained through silylation of LDHs, and their structures, morphologies, bonding mechanisms and thermal stabilities can be readily controlled by changing the experimental parameters during the preparation and drying procedures (with or without surfactant).

Experimental

Chemicals

Magnesium nitrate hexahydrate (min. 99.0%) was purchased from Ajax Finechem. Aluminum nitrate nonahydrate (min. 98.0%), sodium dodecylbenzenesulfate (98.5%), and 3-aminopropyltriethoxysilane (98.5%) were purchased from Sigma-Aldrich. Ethyl alcohol (absolute, 99.5%) was purchased from Merck.

Synthesis of materials

1. Mg₆Al₂(OH)₁₆CO₃·4H₂O (Ht)

LDHs were prepared by co-precipitation, as described by Miyata³¹. With a molar ratio of 3:1 (Mg²⁺/Al³⁺), 9.6 g (37.5 mmol) of Mg(NO₃)₂·6H₂O and 4.7 g (12.5 mmol) of Al(NO₃)₃·9H₂O were dissolved in 44 ml distilled water (Solution A). 4 g (0.1 mol) NaOH were dissolved in 50 ml of distilled water (Solution B). At room temperature, Solution B and Solution A were dropped into 50 ml distilled water with vigorous stirring. The pH value of the mixture was kept at 10 pH units. After filtering, and washing with distilled water, the gel-like product was separated into two batches. One was stored in a sealed container for further reaction (denoted as Ht_w); the other was dried at 75 °C (denoted as Ht).

2. MgAl-Ht_d-Sil (H_d-Si)

With stirring, 0.65 g dried Ht was suspended into 50 ml ethanol and then added drop-wise into 5.0 ml (21.5 mmol) 3-aminopropyltriethoxysilane (APS). After stirring for 6 h, the gel-like product was washed by centrifuge-washing cycles until 500 cm³ was consumed and dried at 75 °C (denoted as H_d-Si).

3. MgAl-Ht_w-Sil (H_w-Si)

About 3.20 g Ht_w (after dried overnight at 75 °C, the mass comes to 0.65 g), was suspended in 50 ml ethanol. Subsequent treatment was as described in step 2, and the resultant materials

was denoted as H_w-Si.

4. MgAl-S_w-Sil (HS_w-Si)

With a molar ratio of 3:1 (Mg²⁺/Al³⁺), 9.6 g of Mg(NO₃)₂·6H₂O and 4.7 g of Al(NO₃)₃·9H₂O were dissolved in 44 ml of distilled water (Solution C). 4 g NaOH and 3.4 g (5.0 mmol) Na-dodecylsulfate (SDS) were dissolved in 100 ml distilled water (Solution D). At room temperature, Solution C, and D were dropped to 50 ml distilled water with vigorous stirring, maintaining the pH value of the mixture at ~10 pH units. The mixture was aged at 80 °C in a water bath for about 12 h, and afterwards, the resultant slurry was filtered, and washed with distilled water. The resultant wet precipitation (HS_w) was suspended in 50 ml ethanol. The mixture was stirred for 30 min before adding 7.0 ml APS. After stirring for another 6 h, the resultant slurry was filtered, and washed with ethanol. The obtained sample was denoted as HS_w-Si.

5. MgAl-SDS-APS (HG-Si)

At room temperature, Solution C, D and 5.0 ml APS (dissolved in 50 ml ethanol) were dropped to 44 ml distilled water with vigorous stirring, maintaining the pH value of the mixture at ~10 pH units. The mixture was aged at 80 °C in a water bath for about 12 h, and afterwards, the resultant slurry was filtered, washed with distilled water, and dried at 75 °C. The obtained material was designated as HG-Si.

Characterization of materials

Infrared spectroscopy

Infrared spectra were obtained using a Nicolet Nexus 870 FTIR spectrometer with a smart endurance single bounce diamond ATR cell. Spectra were obtained over the 4000 to 525 cm⁻¹ range by the co-addition of 64 scans with a resolution of 4 cm⁻¹ and a mirror velocity of 0.6329 cm s⁻¹.

X-ray-diffraction

Powder XRD patterns were recorded using a Bruker D8 Advance diffractometer with Cu Kα radiation (λ = 1.5406 Å), operating at 40 kV and 40 mA. The incident beam was monochromated through a 0.020 mm Ni filter then passed through a 0.04 rad Soller slit, a 1.0 mm fixed mask with 1.0° divergence slit, and a 0.2° anti-scatter slit, between 1 and 76° (2θ) at a scan speed of 1.5° min⁻¹ with an increment of 0.01°.

Infrared emission spectroscopy

Infrared emission spectroscopy (IES) was carried out on a Nicolet spectrometer, which was modified by replacing the IR source with an emission cell. Approximately 0.2 mg samples were spread as thin layers on a 6 mm diameter platinum surface in a N₂ atmosphere. The emission spectra were collected at intervals of 50 °C over the range 100–1000 °C. Considering both precision and time efficiency, the spectra were acquired by co-addition of 1024 scans for the temperature from 100 to 250 °C (about 10 min 34 sec for each time), 128 scans for the temperatures between 300 and 500 °C (about 1 min 19 sec) and 64 scans for the temperatures between 550 and 1000 °C (about 40 sec), with a resolution of 4 cm⁻¹. More detailed descriptions of the cell and principles of the emission experiment are available in the literature^{31, 32}.

Transmission electron microscopy

Transmission electron microscopy (TEM) images were obtained in a JEM-2010HR electron microscope operating at an acceleration voltage of 200 kV. The specimens for TEM

observation were prepared by the following procedure. The clay sample was dispersed in 95% ethanol for 5 min, and then a drop of sample suspension was dropped onto a carbon-coated copper grid, which was left to stand for 10 min and transferred into the microscope.

Solid state ^{29}Si CP/MAS NMR measurement

^1H decoupled solid state ^{29}Si CP/MAS NMR spectra were recorded on a Varian 400-MR NMR spectrometer, operating at 79.43 MHz. Tetramethylsilane (TMS) was used as the external reference with the *tanp* pulse sequence in a 5 mm silicon nitride rotor spinning at 3.5 kHz. Spinal decoupling was used with a contact time of 3 ms. 2000 data points were recorded over a spectral width of 500 ppm. Transients were acquired with a recycle delay of 1 s until sufficient signal-to-noise had been achieved (ranging from -250 to 250 ppm). Data were processed using the Nuts (Acorn NMR, US) software package and peak deconvolution was undertaken using the Jandel 'Peakfit' (SPSS, US) software package. The details of band fitting processes are reported^{26, 29}.

Results and discussion

FTIR spectroscopy

The bond changes between Ht and silylated samples obtained using the different methods were confirmed by FTIR spectroscopy (Figure 1). For Ht (Figure 1a), the O-H related bands are at around 3606 and 3670 (stretching modes of M-OH), 3466 (water), 3314 (H-bonds between -OH and interlayer water) and 3073 cm^{-1} (the bridge bond between H_2O and anions)³². The band corresponding to the water bending mode is observed at $\sim 1636 \text{ cm}^{-1}$. The strong and sharp band at $\sim 1350 \text{ cm}^{-1}$ is due to the ν_3 asymmetric stretching mode of CO_3^{2-} and the 827 cm^{-1} band is assigned to ν_2 modes of the CO_3^{2-} located within interlayer spaces. The bands at 576 cm^{-1} and 547 cm^{-1} are attributed to the M-O stretching vibration (M = Mg^{2+} , Al^{3+}).

Figure 1

The role of water molecule was assessed during the silylation procedure. Dried Ht and water-rich Ht were chosen as substrates to react with APS in ethanol. The spectra of $\text{H}_w\text{-Si}$ (Figures 1b and c) show four main differences from the raw Ht sample. First, the neoformative bands between 1200 and 950 cm^{-1} were recorded. They were assigned to Si-O stretching vibrations from silanes demonstrating the existence of siloxane bridge bonds in silylated samples. In particular, the band at 996 cm^{-1} gives a strong support to the presence of covalent bonds between APS and M-OH of Ht surfaces²⁶. Another silane related change is the appearance of -CH₂ stretching (region 2980-2800 cm^{-1}) together with weak signals at around 1520 cm^{-1} , corresponding to -NH₂ deformation. Meanwhile, the bands present at around 774 and 610 cm^{-1} were assigned to Si-O perpendicular stretching and Si-O-M deformation vibrations, respectively. Important evidence was also observed in the region associated with -OH stretching related modes. The broad and low peak between 3700 and 3300 cm^{-1} was replaced by much narrower and sharper peaks with high intensity. This may be resulted from -OH consumption in the

procedure of condensation between APS and M-OH. All these evidences lead to a conclusion that APS was successfully grafted onto the Ht surface.

When using dried Ht for silylation (Figure 1b), few changes were identifiable for the appearance of silane. While using water-rich Ht (Figure 1c), most vibrations of APS were observed clearly in the spectrum of the product. As mentioned above, in water-rich systems, silane hydrolysis is prior to condensation, while in non-aqueous systems, the silylation procedure may meet with difficulty since there is no hydrolysis of silanes due to lack of water. A resolution is to use silanes with -NH₂ groups for grafting, where the condensation reaction will move towards self-catalysis to form a stable five (or six)-ring intermediates⁷. Since trace amounts of water are necessary to activate the hydrolysis processes at room temperature³³, it is presumed that APS has not been grafted but adsorbed onto the dried Ht surface.

Surfactant also plays an important role during the silylation procedure. Two experiments were designed to assess this effect. The first used the wet gel of surfactant modified Ht (HS_w) to obtain silylated product; the second used *in situ* coprecipitation method to synthesis silylated LDHs^{26, 34}. The cocentration of surfactant was below the critical concentration for intercalation³⁵ in these two cases. The IR spectrum of $\text{HS}_w\text{-Si}$ shows lower intensity than those derived from inorganic substrates. All the vibrations due to APS displayed in $\text{H}_w\text{-Si}$ can also be observed in this sample, except for some overlaps of the bands due to the dodecylsulfate anion at around 1060 cm^{-1} . Furthermore, the vibrations due to C-H are also found in the region of 2960-2850 cm^{-1} and at around 1380 cm^{-1} . The stretching vibrations of -OH group shows a broad peak, indicating more H bonds were formed between the surface hydroxyl groups of Ht, the interlayer anions, and/or water molecule. The sample synthesized by the *in situ* method shows a unique spectrum, particularly in the wavenumber region of 1150-900 cm^{-1} . The vibration located at 1060 cm^{-1} and in the region of 990-950 cm^{-1} , corresponding to stretching modes of Si-O bonded to different atoms (such as C, M and Si)^{26, 35}, shows a sharp peak with higher intensity than the other samples. One explanation may be that the product of the *in situ* method contained more APS³⁶, and more complex condensation products formed during the silylation procedure with the aqueous system used in this case (supported by NMR spectra below).

XRD results

The X-ray diffraction patterns of Ht and its silylated products are shown in Figure 2. The XRD pattern of Ht displays a typical and well ordered layer structure with a basal spacing (d_{003}) of 7.9 Å (Figure 2a). This value matches well with the standard ICDD reference pattern 01-089-0460 (Hydrotalcite, *syn*- $\text{Mg}_6\text{Al}_2(\text{OH})_{16}\text{CO}_3\cdot 4\text{H}_2\text{O}$).

Figure 2

In the case of the silylation reaction without surfactant, the products show narrow, sharp patterns with high intensity in the region of 7-37 ° ((003), (006), and (009)), with d_{001} values very close to those of the raw Ht. In addition, two sharp, symmetric and lower reflections in region 60-63 ° ((110) and (113)) indicate

that the resultant materials are of high crystallinity with well distributed of interlayer anions. The unchanged d spaces show that the silane molecules can only hydrolyze with moisture and condense with the hydroxyl groups on the external surface and/or edge of Ht.

The difference between H_d-Si and H_w-Si is a consequence of the H_w-Si obtained using Ht_w without drying process before silane grafting. In this case, the water adsorbed on the surface of Ht_w can induce APS to hydrolyze and condense with surface hydroxyl groups, so more APS are detected in the products as shown by stronger vibrations in the FTIR spectrum than for H_d-Si. Furthermore, intensified reflections were observed for H_w-Si compared with those in H_d-Si, indicating a higher crystallinity. This may be a result of the extra crystallization time for H_w-Si, considering Ht_w was kept in the wet state.

The influence of surface affinity on the grafted resultants was also investigated by introducing surfactant to improve the hydrophobicity of the Ht surface. The XRD patterns of the resultant materials are shown in Figures 2d and 2e. The d₀₀₃ values are 8.1 Å and 8.0 Å for HS_w-Si and HG-Si, respectively. No reflection was detected at the lower 2 theta angles, suggesting that the silylation reaction only can occur on the external surfaces of LDHs. This is quite different from our previous results³⁰. The reflections become broad and weak in both of the surfactant modified samples, implying that the products are composed of just a few stacked LDH layers with rather lower crystallinity³⁷.

TEM images

The morphologies of silylated products synthesized via different synthesis methods are shown in Figure 3. Similar to the raw Ht, the H-Si obtained by using dried Ht in ethanol medium shows small platelets with smooth surfaces^{26, 34}. While using water-rich Ht_w as substrate, the resultant H_w-Si sample crystals exhibit a rough surface. These provide evidences for the water-inducing-silylation procedure as presumed from XRD and FTIR results. In addition, the crystals of H_w-Si tend to bond with one another. A possible explanation is that APS has three siloxane bonds that can condense with each other as well as being able to condense with surface hydroxyl groups of LDHs. As a result, an intermolecular Si-O-Si linkage matrix is formed between two (or more) adjacent silylated LDHs. A similar phenomenon can also be observed in the surfactant-containing products synthesized via the other two approaches. In the cases, water is available to activate such a condensation. On the contrary, if the reaction occurs in a non-aqueous medium, intermolecular condensation is avoided and only the silylation reaction can take place through a self-catalysis procedure⁷.

Figure 3

The influence of surfactant on the silylated product is significant, as shown in the TEM images of HS_w-Si and HG-Si. The sample of HS_w-Si displays unique fluffy structures and spherical aggregations, while the sample of HG-Si shows large tightly bonded plate-like particles with rough surfaces. Considering the SDS and APS contents are the same throughout the whole reaction, the morphology difference between these two

products is probably resulted from differences in the reaction media. In the case of HS_w-Si, the silylation process occurs in ethanol. The hydrophilic sulfate anions of surfactant molecules associate with the moist surfaces of LDHs while hydrophobic alkyl chains are arrayed outwards radially. As a result of such a distribution, the siloxane head of APS has to approach the surface hydroxyl group of HS_w in a similar manner. Finally, spherical aggregation of HS_w-Si with a fluffy structure is formed. This structure and aggregation is stable and maintained even after being thoroughly stirred in CO₃²⁻ (proceeding work). As for HG-Si, however, the influence of surfactant is not so obvious. The content of SDS used in this case was controlled to minimize its entry into the interlayer space of LDHs³⁵ during the process of nucleation and crystallization. Therefore, most of the DS⁻ are evenly distributed in aqueous solution and crystalline surface. The affinity between APS and surface hydroxyl group of LDHs is driven by the increase of hydrophobicity of the LDHs' surface, modified by DS⁻^{34, 35}. Under these circumstances, the plate-like layer structure observed in raw LDHs is well maintained in the silylated product.

²⁹Si NMR spectroscopy

In order to examine the differences between oligomeric species formed between APS and LDHs described above, the ²⁹Si CP/MAS NMR was used to assess the silylated products (Figure 4). Tⁿ notations (n=0, 1, 2 and 3) are used to describe the different number of "O bridge" structures and the different kinds of siloxane bonds formed between silane and the substrate or the neighboring APS²⁷. The possible products, generated from hydrolysis of APS and condensation between APS and silica in aqueous solution, are discussed in the literature³⁵. The NMR signals of silylated products were assigned, based on the differences in chemical shift and the reaction solvents in comparison with reported values^{27, 35}. The relative populations of each type of siloxane bond are summarized according to peak fitting results (Table 1).

Figure 4

Table 1

Different bonding modes among silanes and between silane and LDHs are observed in the products obtained under different conditions. For a water-free system, no significant signal is observed in the NMR spectrum of the H_d-Si (Figure 4a), implying no bond formation of Si-O-M (M=Al/Mg). This result is consistent with the conclusions made from the IR results. Obvious signals are recorded in the NMR spectra of the two silylated products synthesized via the induced hydrolysis method (Figures 4b, 4c and Table 1). For H_w-Si, in contrast to the previously reported cases^{27, 35}, the hydrolyzed monodentate APS molecule (T¹) was detected as signals at -42.4 and -51.8 ppm and with a high relative population (53.8%). A possible explanation for the observation of a remaining ethoxy group is that ethanol was used to dissolve APS before exposure to the aqueous solution, which could protect APS against hydrolysis³⁶. The

other signals were assigned to two types of hydrolyzed bidentate derived from APS resonance at -58.9 and -61.7 ppm (46.2%), respectively. No tridentate was observed in the NMR spectrum of H_w -Si. When using HS_w as a substrate for the grafting reaction, one signal consistent with hydrolyzed monodentate (-51.7 ppm, 29.7%), two types of hydrolyzed bidentate fashions of APS (-56.9 and -63.7 ppm, 51.5%), and two types of tridentate bonding fashions were observed (-68.3 and -71.5 ppm, 18.8%). The variations between these two products indicate that APS tends to form intermolecular bonding in the presence of DS^- , due to the dual role effect of surfactant in the reaction system³⁵. Surfactant can change the surface of LDHs from hydrophilic to hydrophobic which promotes the approach of silane to the clay surface. Meanwhile, surfactant covers the $-OH$ on the surface of LDHs prior to APS leaving less “free $-OH$ ” available for the silylation reaction. In the reaction system without surfactant, APS is well dispersed and hard to condense with another one, resulting in a higher population of T^1 structure in the products. While the affinity of the substrate is changed by DS^- , more APS is exposed to the surface of LDHs. Since there are not enough free $-OH$ for the silylation reaction, condensation between APS may be improved to form more products with T^2 and T^3 structures. These intermolecular condensations can well explain the aggregations of HS_w -Si as observed in TEM images. This conclusion is further supported by the analysis of the NMR spectrum of HG -Si. The HG -Si was synthesized by the co-precipitation method²⁶, in which water is superfluous to the hydrolysis of APS. The pre-organization of APS molecules would occur before grafting, giving rise to the formation of dimerized chains³⁴. As a result, the populations of hydrolyzed bidentate II (T^2) and tridentate I (T^3) bonding is greatly increased (78.5%). These T^2 and T^3 structures can well explain the tight connections between layers, as observed in TEM images.

IES analysis

The more detailed spectroscopic character of silylated samples were investigated by infrared emission spectroscopy analysis. The thermal decomposition of the samples can be clearly revealed by the spectroscopic changes during heating process³⁰.

Figure 5

Figure 6

IES spectra of H_d -Si (Figure 5) shows a rapid loss of intensity in the region of 3500 – 3000 cm^{-1} as the temperature was increased up to 150 °C, corresponding to two DTG peaks as shown in Figure S1a with a mass loss of about 13.2%. This is attributed to the loss of ethanol absorbed on the surface of LDHs. Meanwhile, IES peaks due to APS are decreased in intensity, consistent with the scissoring vibration of $-NH_2$ (1580 cm^{-1}), and $Si-CH_2$ (1580 cm^{-1}) etc.. Compared with the FTIR spectrum of H_d -Si, two new vibrations were displayed in IES spectra, located at 1180 – 980 cm^{-1} and attributed to $Si-O$ related vibrations. In particular, the vibration at 994 cm^{-1} , which is assigned to $Si-O-M$ ($M=Al$ and Mg) related bonds^{26, 29, 30, 35} indicating that covalent bonds

are formed between APS and LDHs during the heating process. This observation shows that temperature is a very important parameter during the silylation reaction and is necessary for the silylation reaction in non-aqueous media⁷. The vibrations due to surface $-OH$ of LDHs and $-CH_2$ of APS disappeared gradually as the temperature elevated to 600 °C, related to a main mass loss stage (27.7%) and a small one (4.7%) as indicated in Figure S1a (Electronic supplementary information, ESI). During this procedure, the vibration at 1347 cm^{-1} disappeared at around 350 °C, a sign of volatilization of interlayer CO_3^{2-} . With further temperature increased, a series of IES spectral bands, corresponding to Si bonded to different atoms were clearly displayed at 1511 , 1424 , 1190 – 980 and 855 cm^{-1} etc. The bands at 1511 and 1424 cm^{-1} were ascribed to the overtone of $Si-O$ and $Si-O-Si$ symmetric stretching modes and the bands at 1186 and 858 cm^{-1} were ascribed to the stretching modes of $Si-O-Si$ and $M-(Si-O)_n-M$, respectively. These bonds are distinguishable even when temperature increases to 1000 °C. The appearance of these bands indicates that the silicate/silica phase is formed during the heating procedure.

Figure 7

Figure 8

The IES spectra of H_w -Si (Figure 6) were similar to those of H_d -Si, except for some peak shifts and intensity variations, and the vibrations due to APS (e.g. 3350 – 3280 cm^{-1} corresponding to $-NH_2$ stretching, 2930 – 2850 cm^{-1} to $-CH_2$ stretching, 1580 cm^{-1} to $-NH_2$ scissoring and 1120 – 1000 cm^{-1} to $Si-O$ related stretching) showed much higher intensity. These differences imply that more APS bond with LDHs plates in H_w -Si. Furthermore, the vibrations of H_w -Si located at 1160 – 1400 cm^{-1} are less clear like those observed for H_d -Si, while the vibrations located at 1000 – 850 cm^{-1} are much more distinct. This indicates different bonding mechanisms in the two samples at the temperatures above 400 °C.

The spectroscopic characteristics of HS_w -Si and HG -Si are also (Figures 7 and 8) show the presence of DS^- and the changes with heating, including the vibrations at around 2960 – 2850 cm^{-1} ($C-H$ stretching), 1370 cm^{-1} ($-CH_2-$ wagging), 1205 cm^{-1} and 1056 cm^{-1} ($-OSO_3^-$ stretching). All the $C-H$ related vibrations disappeared at around 600 °C, accompanying with the loss of surface $-OH$. When the temperature is above 250 °C, the bond at around 1157 cm^{-1} in HG -Si sample appears with the disappearance of $-OSO_3^-$ stretching³⁰. Similarly to those in H_w -Si and H_d -Si, the $Si-O$ related vibrations and their overtones are recorded above 400 °C in the HS_w -Si and HG -Si. The presence of these bonds suggests a higher thermal stability in all the silylated products than those in pristine LDHs. The related details of TG/DTG curves can be found in the ESI

Conclusions

Four approaches have been designed to investigate the effect of the state of substrate, solvent, and surfactant on the structure, morphology, bonding mechanisms, and thermal stability features

of silylated products. The characterization results show that the directly silylation reaction cannot occur between the dried LDHs and APS in ethanol medium. However, during heating, the condensation reaction takes place between the adsorbed APS and LDHs plates. While using wet state substrates with and without surfactant in ethanol solvent, the silylation process can be induced by hydrolysis of APS on the surface of LDHs plates, as it is with the silylation reaction in the water medium. The morphology of H_d-Si particles shows smooth surfaces similar to those of LDHs, while H_w-Si particles show a rough surface. Surfactant plays dual role during the silylation process. On one hand, surfactant improves the hydrophobicity of the LDHs during the process of nucleation and crystallization, resulting in fluffy shaped crystals in HS_w-Si; on the other hand, they occupy the surface -OH and leave less "free -OH" available for the silylation reaction, favoring formation of silylated products with higher populations of hydrolyzed bidentate (T²) and tridentate (T³) bonding in both HS_w-Si (70.3%) and HG-Si (94.5%). This bonding leads to spherical aggregation and tightly bonded particles in HS_w-Si and HG-Si, respectively. All silylated products show higher thermal stability than those of pristine LDHs.

Acknowledgement

The financial and infra-structure supports of the National Science Fund for Distinguished Young Scholars (Grant No. 40725006) and for Young Scientists (Grant No. 41002015), and National Natural Science Foundation of China (Grant No. U0933003). are acknowledged. The financial and infra-structure support of the Queensland University of Technology Inorganic Materials Research Program of the Chemistry Discipline is gratefully acknowledged. The Australian Research Council (ARC) is thanked for funding.

Notes and references

^a Guangzhou Institute of Geochemistry, Chinese Academy of Sciences, Guangzhou 510640, P. R. China

^b Chemistry Discipline, Faculty of Science and Technology, Queensland University of Technology, Brisbane Queensland 4001, Australia

* Author to whom correspondence should be addressed (hehp@gig.ac.cn or r.frost@qut.edu.au)

† Electronic supplementary information (ESI) available: TG/DTG analysis.

1. R. L. Frost and E. Mendelovici, *Journal of Colloid and Interface Science*, 2006, **294**, 47-52.
2. G. J. Kluth, M. M. Sung and R. Maboudian, *Langmuir*, 1997, **13**, 3775-3780.
3. E. Mendelovici and R. L. Frost, *Journal of Colloid and Interface Science*, 2005, **289**, 597-599.
4. E. Mendelovici, R. L. Frost and J. T. Klopogge, *Journal of Colloid and Interface Science*, 2001, **238**, 273-278.
5. P. G. Pape and E. P. Plueddemann, *Journal of Adhesion Science and Technology*, 1991, **5**, 831-842.
6. H. Tegelstroem and P. I. Wyoeni, *Electrophoresis*, 1986, **7**, 99.

7. P. VanDerVoort and E. F. Vansant, *Journal of Liquid Chromatography & Related Technologies*, 1996, **19**, 2723-2752.
8. S. O'Leary, D. O'Hare and G. Seeley, *Chemical Communications*, 2002, 1506-1507.
9. F. Wypych and K. G. Satyanarayana, *Journal of Colloid and Interface Science*, 2005, **285**, 532-543.
10. A. Y. Park, H. Kwon, A. J. Woo and S. J. Kim, *Advanced Materials*, 2005, **17**, 106-109.
11. F. Wypych, A. Bail, M. Halma and S. Nakagaki, *Journal of Catalysis*, 2005, **234**, 431-437.
12. C. Li, G. Wang, D. G. Evans and X. Duan, *Journal of Solid State Chemistry*, 2004, **177**, 4569-4575.
13. G. Kickelbick, *Hybrid Materials: Synthesis, Characterization, and Applications*, Wiley-VCH, 2007.
14. F. Cavani, F. Trifiro and A. Vaccari, *Catalysis Today*, 1991, **11**, 173-301.
15. N. D. Hutson, S. A. Speakman and E. A. Payzant, *Chemistry of Materials*, 2004, **16**, 4135-4143.
16. E. D. Dimotakis and T. J. Pinnavaia, *Inorganic Chemistry*, 1990, **29**, 2393-2394
17. Y. W. You, H. T. Zhao and G. F. Vance, *Journal of Materials Chemistry*, 2002, **12**, 907-912.
18. C. Domingo, E. Loste and J. Fraile, *Journal of Supercritical Fluids*, 2006, **37**, 72-86.
19. B. M. Choudary, N. S. Chowdari, K. Jyothi and M. L. Kantam, *Journal of the American Chemical Society*, 2002, **124**, 5341-5349.
20. M. C. Hermosin, I. Pavlovic, M. A. Ulibarri and J. Cornejo, *Water Research*, 1996, **30**, 171-177.
21. S. Angloher, J. Kecht and T. Bein, *Chemistry of Materials*, 2007, **19**, 5797-5802.
22. M. D. K. Ingall, C. H. Honeyman, J. V. Mercure, P. A. Bianconi and R. R. Kunz, *Journal of The American Chemical Society*, 1999, **121**, 3607-3613.
23. H. Lee, S. M. Dellatore, W. M. Miller and P. B. Messersmith, *Science*, 2007, **318**, 426-430.
24. S. Oh, T. Kang, H. Kim, J. Moon, S. Hong and J. Yi, *Journal of Membrane Science*, 2007, **301**, 118-125.
25. Y. R. Yeon, Y. J. Park, J. S. Lee, J. W. Park, S. G. Kang and C. H. Jun, *Angewandte Chemie-international Edition*, 2008, **47**, 109-112.
26. Q. Tao, H. P. He, R. L. Frost, P. Yuan and J. X. Zhu, *Applied Surface Science*, 2009, **255**, 4334-4340.
27. J. W. Dehaan, H. M. Vandenbogaert, J. J. Ponjee and L. J. M. Vandeven, *Journal of Colloid and Interface Science*, 1986, **110**, 591-600.
28. A. Dkhissi, A. Esteve, L. Jeloica, D. Esteve and M. D. Rouhani, *Journal of The American Chemical Society*, 2005, **127**, 9776-9780.
29. Q. Tao, J. Zhu, R. L. Frost, T. E. Bostrom, R. M. Wellard, J. Wei, P. Yuan and H. He, *Langmuir*, 2010, **26**, 2769-2773.
30. Q. Tao, H. He, R. Frost, P. Yuan and J. Zhu, *Journal of Thermal Analysis and Calorimetry*, 2010, **101**, 153-157.
31. S. Miyata, T. Kumura and M. Shimada, German, 1970.

32. J. T. Kloprogge, L. Hickey and R. L. Frost, *Journal of Raman Spectroscopy*, 2004, **35**, 967-974.
33. A. V. Kiselev and V. I. Lygin, *Infrared spectra of surface compounds*, John Wiley & Sons, New York, 1975.
- 5 34. J. X. Zhu, P. Yuan, H. P. He, R. Frost, Q. Tao, W. Shen and T. Bostrom, *Journal of Colloid and Interface Science*, 2008, **319**, 498-504.
35. Q. Tao, J. Yuan, R. L. Frost, H. He, P. Yuan and J. X. Zhu, *Applied Clay Science*, 2009, **45**, 262-269.
- 10 36. S. R. Culler, H. Ishida and J. L. Koenig, *Journal of Colloid and Interface Science*, 1985, **106**, 334-346.
37. G. Hu, N. Wang, D. O'Hare and J. Davis, *Journal of Materials Chemistry*, 2007, **17**, 2257-2266.

Table 1 Solid state ^{29}Si CP/MAS NMR chemical shifts (ppm), the peak assignments of oxane bonds, and relative population of oxane types for the silylation products synthesized via an induced hydrolysis method.

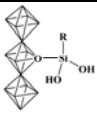
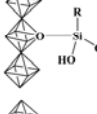
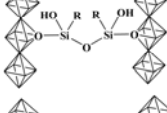
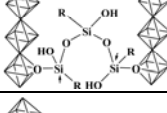

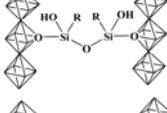
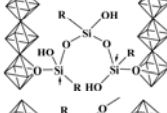
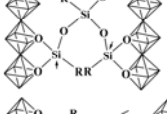
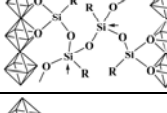

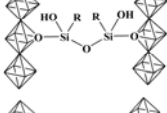
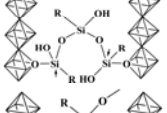
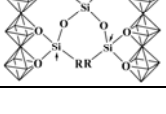
Samples	Chemical shift (ppm)	Peak width (ppm)	Area (%)	Assignments	Notation	Schemes
$\text{H}_w\text{-Si}$	-42.4	2.9	5.4	Hydrolyzed Monodentate I	T^1	
	-51.8	12.3	48.4	Hydrolyzed Monodentate II ²⁹	T^1	
	-58.9	2.8	5.4	Hydrolyzed Bidentate I ²⁹	T^2	
	-61.7	5.7	40.8	Hydrolyzed Bidentate II	T^2	
$\text{HS}_w\text{-Si}$	-51.7	6.4	29.7	Hydrolyzed Monodentate II ²⁹	T^1	
	-56.9	5.3	17.6	Hydrolyzed Bidentate I ²⁹	T^2	
	-63.7	8.5	33.9	Hydrolyzed Bidentate II	T^2	
	-68.3	3.1	2.7	Tridentate I ²⁹	T^3	
	-71.5	5.7	16.1	Tridentate II	T^3	
HG-Si	-53.9	3.2	5.5	Hydrolyzed Monodentate II ²⁹	T^1	
	-58.8	6.1	16.0	Hydrolyzed Bidentate I ²⁹	T^2	
	-62.3	3.3	43.0	Hydrolyzed Bidentate II	T^2	
	-67.8	6.7	35.5	Tridentate I ²⁹	T^3	

Figure captions

Figure 1. FTIR spectra of grafted LDHs: a. Ht, b. H_d-Si, c. H_w-Si, d. HS_w-Si and e. HG-Si.

5

Figure 2. Powder X-ray diffraction patterns of the silylation samples: a. Ht, b. H_d-Si, c. H_w-Si, d. HS_w-Si and e. HG-Si. (The reference patterns and codes are from the ICDD).

10

Figure 3. TEM images of Silylated LDHs: a. H_d-Si, b. H_w-Si, c. HS_w-Si and d. HG-Si.

Figure 4. ²⁹Si NMR spectra of Silylated LDHs: a. H_d-Si, b. H_w-Si, c. HS_w-Si, and d. HG-Si.

15

Figure 5. IES spectroscopy of H_d-Si.

20 **Figure 6.** IES spectroscopy of H_w-Si.

Figure 7. IES spectroscopy of HS